

Properties of a differential pressure pseudospark device

S. K. Karkari,^{a)} S. Mukherjee, and P. I. John
FCIPT, Institute for Plasma Research, Gandhinagar-382044, India

(Received 11 January 1999; accepted for publication 14 October 1999)

A differential pressure pseudospark device is developed to produce a discharge at a pressure of 10^{-4} mbar near the anode. This pressure range is two orders in magnitude lower than conventional pseudospark devices. In this device a pressure gradient is maintained between the cathode and the anode by providing a gas flow through the discharge column. The pressure gradient helps in shifting the Paschen curve more towards the left in comparison to the conventional case. The empirical relationship $V \propto (p^2 d D)^{-2}$, valid without a gas flow, is not applicable when the pressure difference between the cathode and the anode is over two orders in magnitude. Self-biasing collector technique reveals the presence of energetic electrons (0.4–1.2 keV) present in the plasma downstream of the anode. The nature of this plasma at two distinct pressure ranges of operation of the device shows marked difference in properties. A qualitative discussion is presented that explains the possible discharge mechanism in this device. © 2000 American Institute of Physics.

[S0034-6748(00)03301-3]

I. INTRODUCTION

A pseudospark device takes advantage of the hollow cathode effect in producing a discharge towards the left-hand branch of the Paschen curve. The discharge is characterized by the formation of high current densities over short time duration. The temporal evolution of the discharge passes through different states.^{1,2} When sufficient energy is delivered to the electrode system then high-density electron beam can be extracted from a small hole drilled in the anode.³⁻⁷ The operating pressure regime of this discharge is typically higher than 10^{-2} mbar.¹⁻⁴ The electron beam generated by this simple method finds a large number of applications.⁵⁻⁷ However, application of this device, such as in interaction with materials in high vacuum environment (10^{-4} mbar) will require a differential pumping arrangement between the device and the interaction region (IR). This limits the application to the operating pressure range of the device.

It is possible to achieve a differential pressure by reducing the anode-hole size (i.e., by decreasing the conductance of the discharge column) while pumping from the side of the IR. However, drastic reduction of the anode hole size will limit the extraction of energetic species from the device. An alternative approach to this problem is to operate the device itself in a pressure range, identical with the pressure of the interaction region, without actually modifying the device.

In order to operate the device at sufficiently low pressure (less than 10^{-2} mbar) with ionization mean free path for electrons exceeding several times the system dimension will require additional source for ionization. This is possible to achieve by injecting externally produced electrons from a pre-discharge⁸ or by a surface flashover leading to ionizing energetic photons inside the hollow cathode. The primary electrons injected into the discharge column can bring down the E/p (E =electric field; p =pressure) ratio required for

breakdown. All the above methods require an external power source for producing the primary electrons necessary for breakdown.

Another approach to the above problem is to maintain a differential pressure across the length of the discharge column itself. This can be achieved by a simple mechanism of gas flow. In one of the reported experiment,⁹ the gas was introduced from the backspace of the cathode and pumped down from the anode side. In this case the pressure near the cathode will be much higher than the pressure near the anode (since the gas is pumped from the anode side). This leads to a pressure gradient along the discharge column. However, the operating pressure range that was measured near the anode was in the conventional pseudospark pressure range.³⁻⁵ Furthermore, there no report exists on the effect of pressure gradient on the properties of the discharge. The differential pressure pseudospark device (DPPD) adopts this principle in producing a large pressure gradient (about two orders of magnitude) along the discharge column. This is achieved by introducing the gas from the backspace of the cathode and pumped down through the small conductance of the discharge column from the anode side. In this case the pressure along the discharge column will not be uniform as compared to conventional pseudospark devices where the gas feed and the pumping is done from the anode side.³⁻⁵ In DPPD, this pressure gradient along the discharge column helps in providing a pressure range identical to normal pseudospark discharge near the cathode, whereas the pressure near the anode remains low at 10^{-4} mbar. With this configuration, the required breakdown voltage of the gas at sufficiently low pressure near the anode (10^{-4} mbar) is reduced, without any aid from an external ionization source. The article reports on the properties of DPPD, which is operated as an alternative method to obtain the discharge at sufficiently low pressure near the anode.

^{a)}Electronic mail: fcipi@plasma.ernet.in

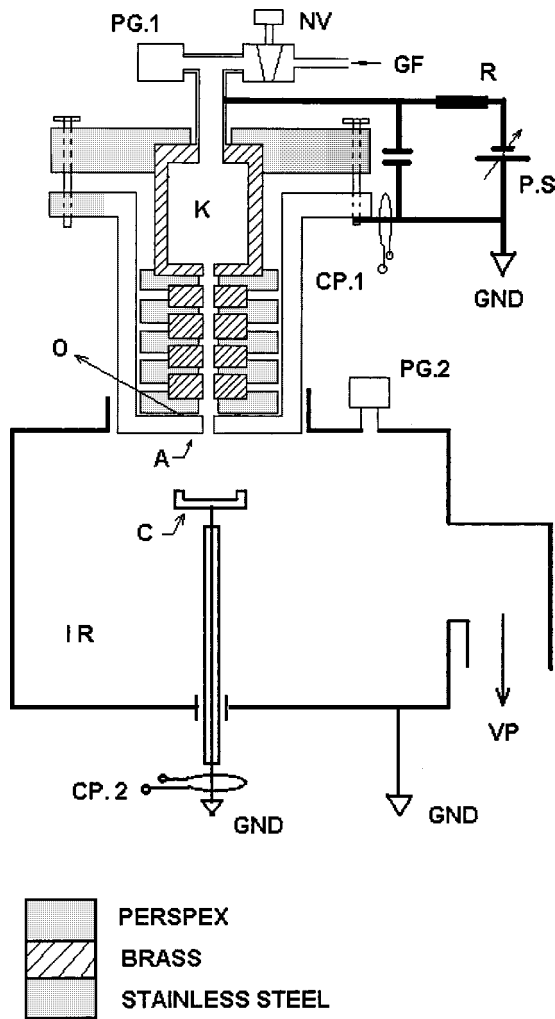


FIG. 1. Schematic of differential pressure pseudospark device. GF=gas feed, NV=needle valve, PG.1=pressure gauge for measuring pressure near anode, PG.2=pressure gauge for measuring pressure near cathode, K=cathode, A_n =anode, O="O" ring, C=collector, VP=vacuum pump, PS=power supply, R=current limiting resistor, CP.1=current probe (discharge current), CP.2=current probe (for measuring current near the downstream of the anode), GND=ground, and IR=interaction region.

Section II describes the experimental setup, diagnostics, and the design of the device. The experimental results are presented in Sec. III. The results are discussed in Sec. IV.

II. EXPERIMENTAL SETUP

A. Differential pressure pseudospark device

The schematic of the device is shown in Fig. 1. The device is comprised of a hollow cathode "K" and a disk shaped anode " A_n " with a central axial hole with dimension⁴ as mentioned in Fig. 2. The gap between the cathode and the anode is comprised of brass and Perspex disks alternately stacked together with "O" rings in between for vacuum tightness. This arrangement capacitively divides the voltage across the gap. The A_n -K gap is adjustable by varying the number of intermediate brass and Perspex disks. The gas is introduced from the cathode backspace and controlled with a precision needle valve. The pressure near the anode is measured with a set of Pirani and Penning gauges and the same is measured behind the cathode from where the

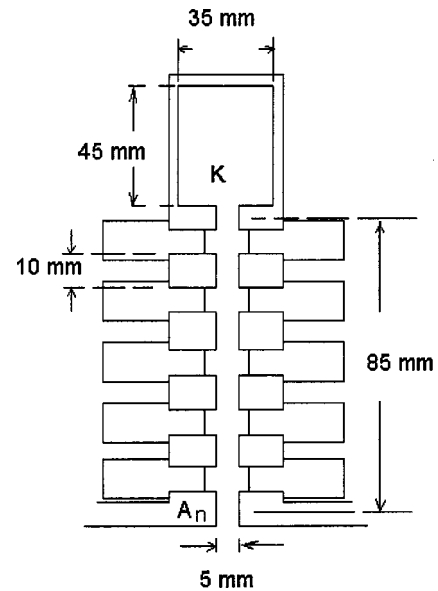


FIG. 2. Dimensions of the differential pressure pseudospark device.

gas is introduced inside the discharge column. In this way the differential pressure is mapped for the system. Figure 3 shows the mapped pressure values for four inter-electrode configurations.

B. Electrical circuits and diagnostics

The electrical circuitry is schematically shown in Fig. 1. For the experiment $C=40$ nF (inductance=20 nH) a single Maxwell capacitor (100 kV) is used. The voltage is applied to the discharge electrodes by slowly varying the input primary voltage of a 20 kV, 250 mA transformer. The breakdown voltage is measured using a Tektronix make high voltage probe (P 6015) with a bandwidth of 75 MHz. The currents are measured using Pearson make current probes (model-411). A movable disk shaped titanium collector (diameter=40 mm) acting as a probe is placed downstream of the anode. The collector is kept grounded for measuring the current. The energy distribution of the charged species is

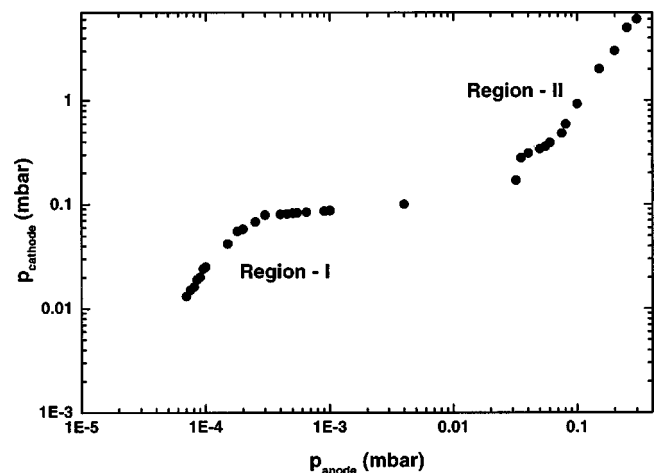


FIG. 3. Differential pressure plot; P_{anode} =pressure measured using PG.1 near anode; $P_{cathode}$ =pressure measured using PG.2 near cathode.

TABLE I. Knudsen's number for the estimate of gas flow through the device, a is the diameter of the discharge column and λ_{mfp} is the mean free path of the gas atoms.

$\lambda_{mfp}/a < 1$	Viscous flow range
$\lambda_{mfp}/a > 1$	Molecular flow range
$0.01 < \lambda_{mfp}/a < 1.00$	Transition flow range

obtained by self-biasing the collector by grounding through noninductive carbon film resistances. The wave forms are captured using a Tektronix make digital storage oscilloscope (DSO) (TDS 320); bandwidth 100 MHz, 500 M Sa/S and are then transferred to the computer.

III. EXPERIMENTAL RESULTS

A. Differential pressure

Figure 3 shows a plot of the pressures measured at two ends of the discharge column by varying gas feed from the backspace of the cathode. The pressures indicated along the x axis are the pressures that are measured near the anode using pressure gauge PG.1. The corresponding pressures measured near the cathode using pressure gauge PG.2 are plotted along the y axis. Due to a significant difference in pressure at the two ends of the discharge column, the flow condition continuously varies from molecular, transition, and viscous range. Depending on the type of flow through the discharge column, the curve is broadly classified into two regions. Region I is identified for a pressure range below 10^{-3} mbar while Region II corresponds to a pressure range above 10^{-3} mbar. An estimate about the type of flow is obtained from the Knudsen number¹⁰ as shown in Table I.

Figure 4 shows the Paschen curve for the two regions described above. The flow conditions at the two ends of the discharge column for three arbitrary points in the Paschen curve are listed in Tables II and III. Table II corresponds to Region I and Table III corresponds to Region II of the Paschen curve. The figures indicate the flow regime along the discharge column at different points in the Paschen curve. The type of flow is almost molecular in Region I, whereas Region II is characterized by a mixed type of flow along the discharge column.

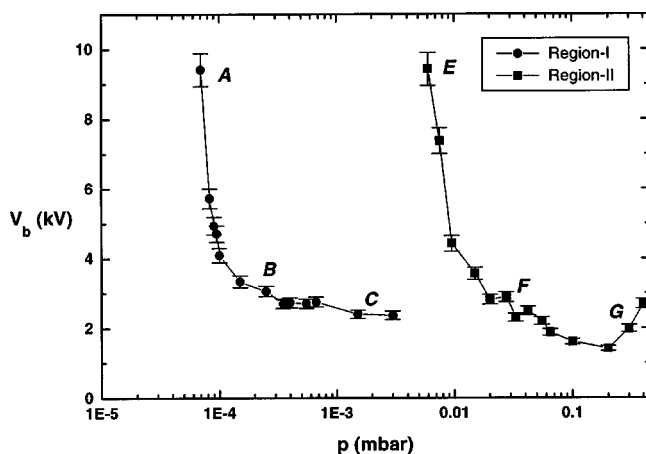


FIG. 4. Paschen's curve; p =pressure measured near the anode, V_b =breakdown voltage.

TABLE II. Flow condition near the cathode and the anode for three different points in Region I of the Paschen curve.

Points	A		B		C	
	λ_{mfp} (m)	Type of flow	λ_{mfp} (m)	Type of flow	λ_{mfp} (m)	Type of flow
Near anode	1.5	mol.	1.16	mol.	0.13	mol.
Near cathode	$8e-3$	mol.	$4e-3$	mol.	$1.25e-3$	trans.

(apprx.)

B. Electrical properties of the discharge

The characteristic discharge voltage and current for two different regions of the Paschen curve are shown in Figs. 5 and 6. The discharge current and the voltage in each of these regions undergo a damped oscillation. The ringing discharge current is partly due to external circuit parameters and partly due to time varying inductance and resistance of the discharge. In this case the resistance of the circuit, $R(5 \text{ m}\Omega) < 2\sqrt{L/C}$. Thus the discharge current rings before it damps to zero. This means that the electron motion along the discharge column changes its direction after each half cycle. In this case the negative peak of the discharge current indicates the electron motion towards the anode. The current signal obtained at the grounded electrode placed at 20 mm downstream from the anode shows a negative going signal (electron current) that corresponds to the negative peak of the discharge current. The current signals decay in magnitude in succession, as the oscillatory discharge current decays with time.

C. Properties of the electron current obtained at the grounded collector

In Region I of the operating pressure regime, the initial electron current signal at the grounded collector is much smaller than successive current signals (Fig. 5). In Region II this is comparatively much larger in magnitude than in Region I (Fig. 6). A positive ion current at the grounded collector is also observed (Fig. 7) when the collector is placed very close to the anode (10 mm). This indicates the possibility of the grounded collector transiently behaving as the anode¹¹ or it is due to ion current from the plasma reaching the electrode.

The multiple electron current pulses at the grounded collector are designated as first, second, third, etc. depending on their order of occurrence in a single discharge. Figures 8 and 9 show the plot of these peak values as a function of collector distance from the anode. The first electron current pulse in Region I is present only at a distance of 20 mm from the

TABLE III. Flow condition near the cathode and the anode for three different points in Region II of the Paschen curve.

Points	E		F		G	
	λ_{mfp} (m)	Type of flow	λ_{mfp} (m)	Type of flow	λ_{mfp} (m)	Type of flow
Near anode	0.014	mol.	$1.05e-3$	Trans.	$3.5e-4$	Trans.
Near cathode	$8e-4$	Trans.	$1.14e-4$	Trans.	$1.75e-5$	Visc.

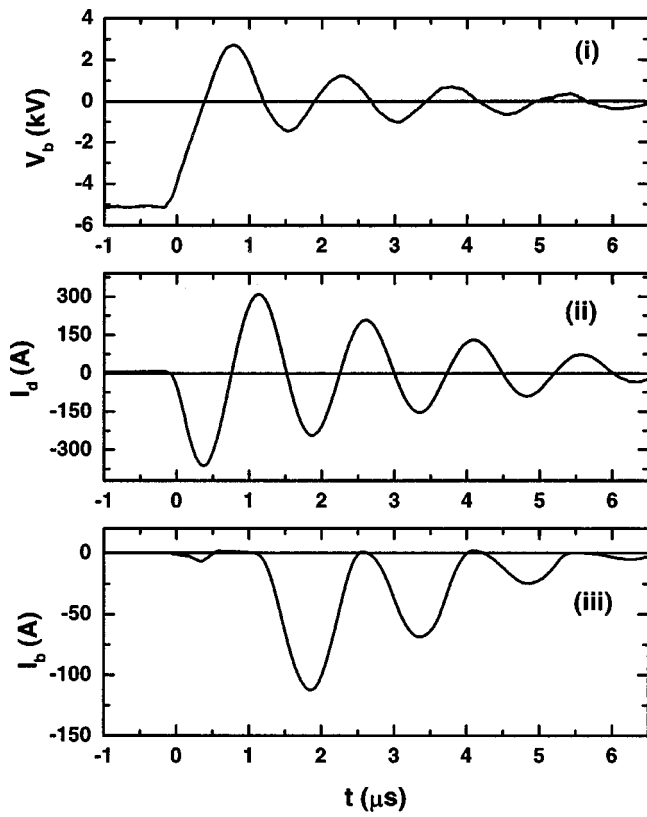


FIG. 5. (i) V_b =breakdown voltage, (ii) I_d =discharge current, and (iii) I_b = electron current for Region I of the Paschen curve.

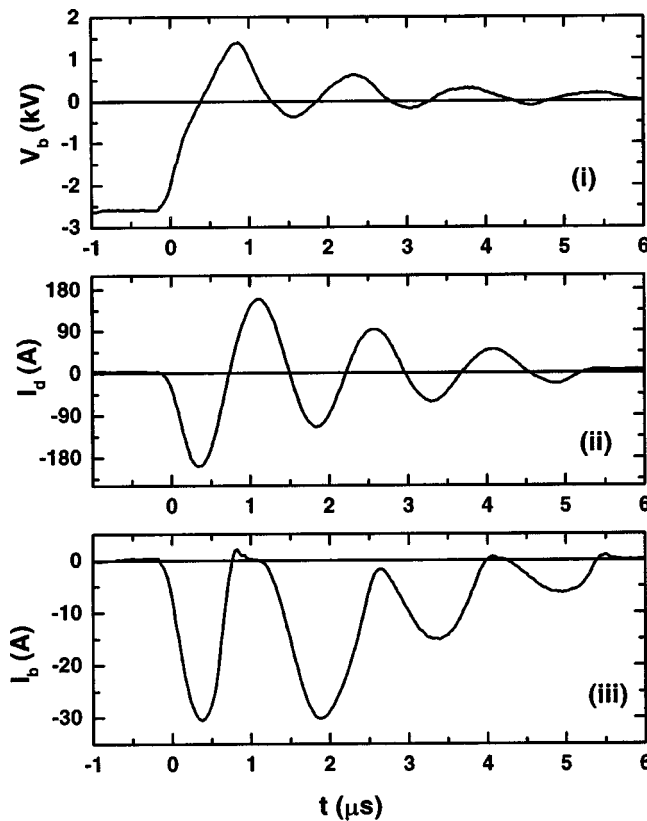


FIG. 6. (i) V_b =breakdown voltage, (ii) I_d =discharge current, (iii) I_b = electron current for Region II of the Paschen curve.

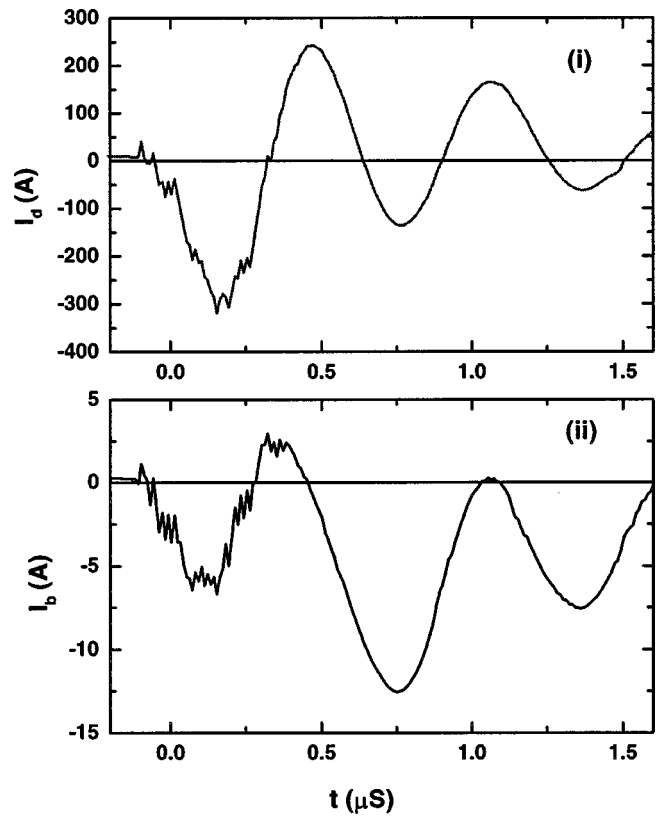


FIG. 7. (i) Typical discharge current wave form, (ii) current collected by the grounded collector for Region I at a distance of 10 mm from the anode. $C_{\text{external}} = 10 \text{ nF}$.

anode (Fig. 8). Whereas in Region II, (Fig. 9) this is observed even when the collector is placed at a distance of 120 mm downstream from the anode. Furthermore, the magnitude of the current pulses that has originated earlier decays faster in comparison to the following pulses with increasing collector distance from the anode.

D. Energy distribution of the electron current at the grounded collector

In order to confirm that the measured current peaks correspond to energetic electrons emitted from the device and to obtain an estimate of the energy distribution that constitutes

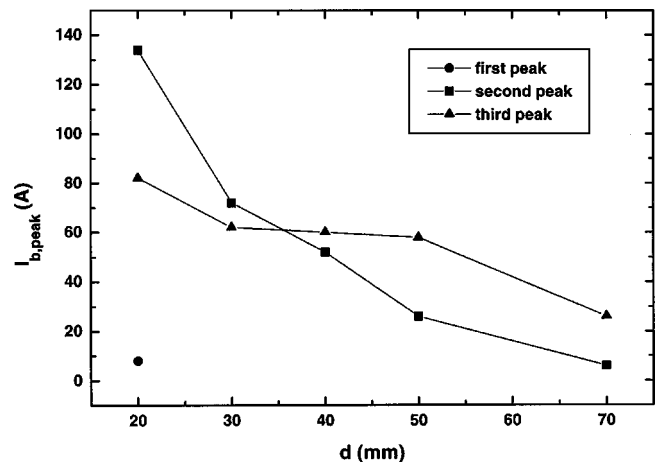


FIG. 8. Fall of peak values of electron current, $I_{b,peak}$ for Region I of the Paschen curve with increasing collector distance, d from the anode.

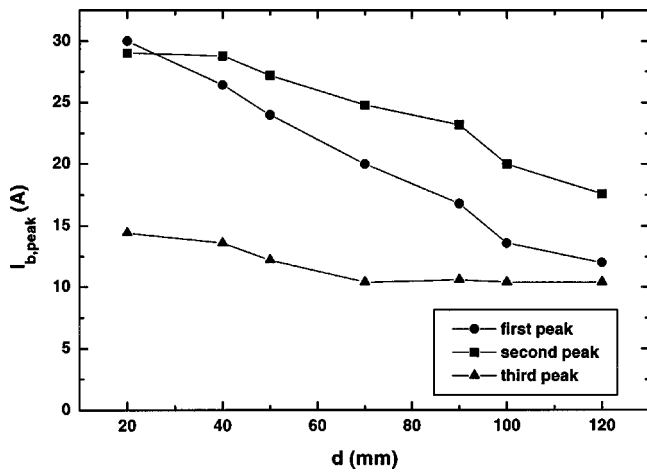


FIG. 9. Fall of peak values of electron current, $I_{b,peak}$ for Region II of the Paschen curve with increasing collector distance, d from the anode.

the current at the grounded collector, a self-biasing collector technique is used.¹² In this case the collector is grounded through various noninductive resistances. The maximum electron current is obtained when the collector is directly connected to the ground through flat copper strips having negligible resistance (less than 5 mΩ). When grounded through resistance, the electron current reduces in magnitude and correspondingly a negative voltage appears across the resistor. Figure 10 shows the fall of second peak of beam current for Region I as a function of external resistance in the circuit. From this curve dI_b/dV is estimated. Here, ‘ I_b ’ is the current collected by the collector and $V = (\int I_b dt / \int dt) \times R$ is the self-biased potential of the collector with respect to the ground. Here the integration is over the total duration of the current pulse. From this estimation the distribution function ‘ $f(E)$,’ is evaluated using established techniques^{13,14} as shown in Fig. 11. Here $E = eV$, is the energy of the electrons. The distribution curve indicates the presence of energetic electrons having significant spread in energies. A major part of the current is comprised of slow electrons having energy up to 400 eV. The maximum energetic electrons constituting the current are approximately 1.2

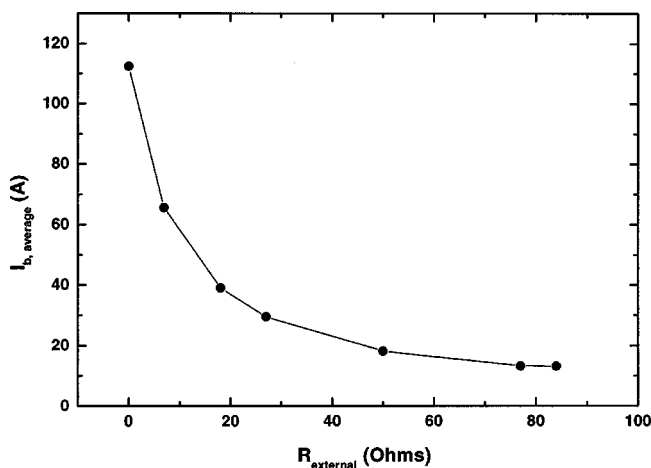


FIG. 10. Fall of average electron current, $I_{b,average}$ with external resistance $R_{external}$ in the circuit.

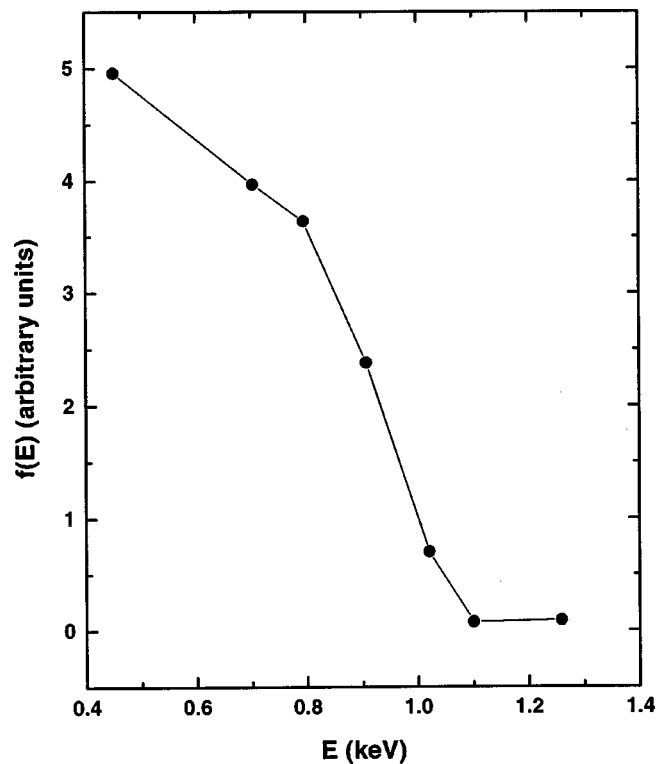


FIG. 11. Energy distribution $f(E)$ of the second peak of electron current for Region I of the Paschen curve. $V_{self-bias}$ = approximate voltage of the energetic species developed across the resistor.

keV. This value corresponds to the maximum energy of the electrons, as the collector cannot be biased more than this value using self-biasing technique.

IV. DISCUSSION

A. The role of differential pressure in discharge formation

Unlike a conventional pseudospark device, the gas flow is varying along the discharge column. Since flow conditions are varying, the E/p ratio will also vary along the length of the discharge column. Thus it is more likely that the discharge initiates in the region where the E/p ratio is minimum. This initial discharge can provide the necessary primary electrons required for ionization at low pressure near the anode. In the same setup, the discharge was not obtained at a pressure of 10^{-4} mbar near the anode when the gas was introduced from the anode side. However, discharge was obtained when the pressure near the anode was much higher (0.1 mbar). This shows that flow of gas through the discharge column is necessary to obtain a discharge at very low pressure near the anode. This is possible only if the gas is introduced from the backspace of the cathode and pumped from the anode side.

The empirical formula¹⁵ for a multi-gap pseudospark device (in the conventional pseudospark pressure range and in the absence of a gas flow) is given by

$$V = \frac{2}{(p^2 d D)^2}; \quad \text{for } h/D > 1.$$

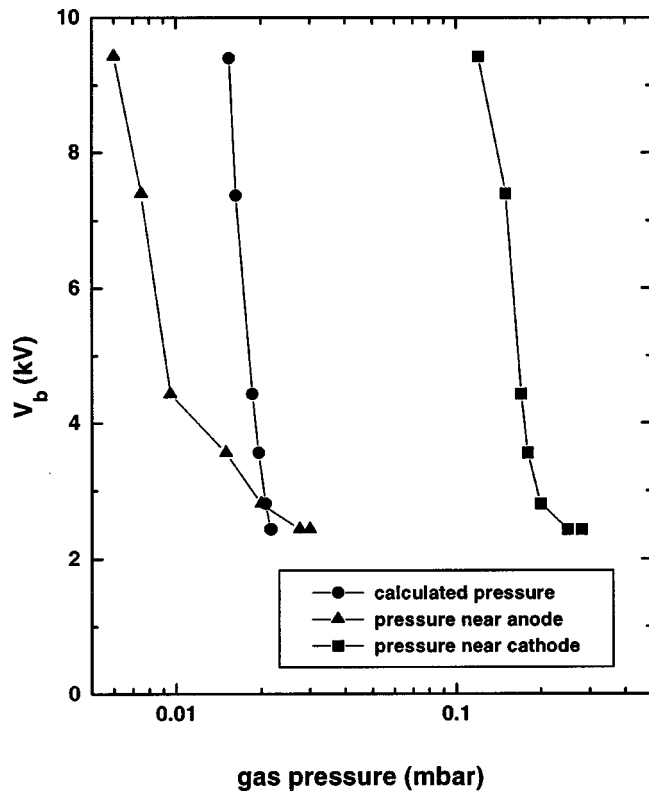


FIG. 12. Left-hand branch for Region II of the Paschen curve.

Here breakdown voltage “ V ” is expressed in kV, pressure “ p ” is expressed in Torr, anode–cathode gap “ d ,” depth “ h ,” and the diameter of the hollow cathode are expressed in mm, respectively. In the present case $h/D=1.2 > 1$, $d \approx 85$ mm, $D=35$ mm. Using this formula, pressure p is calculated from the breakdown voltages, for each region in the left-hand branch of the Paschen curve. The breakdown voltages are then simultaneously plotted for these calculated pressures, pressures measured by PG.1 and PG.2, separately for Regions I and II of the Paschen curve as shown in Figs. 12 and 13.

The calculated pressure using this empirical formula corresponds to the maximum voltage across the gap. In the case of DPPD, the pressure is continuously decreasing in magnitude from the cathode towards the anode. Thus at a given distance d from the cathode, the calculated pressure should correspond to the maximum voltage available at that electrode (before breakdown). Since the formula is arrived at in the case where the gas flow is absent, the average pressure in this case is assumed to lie closer to the anode.

In Fig. 12, the calculated pressures (Region II) lie closer to the pressures that are measured near the anode. Furthermore, the slopes of these curves are almost identical. This indicates some resemblance in the properties of the discharge with the case when there is no gas flow. An electron current pulse at the grounded collector is also observed that corresponds to the initial peak of the discharge current (Fig. 6) and is similar to the conventional pseudospark devices.¹⁶ However, the calculated pressure does not exactly match the measured pressure values near the anode. The reason may be

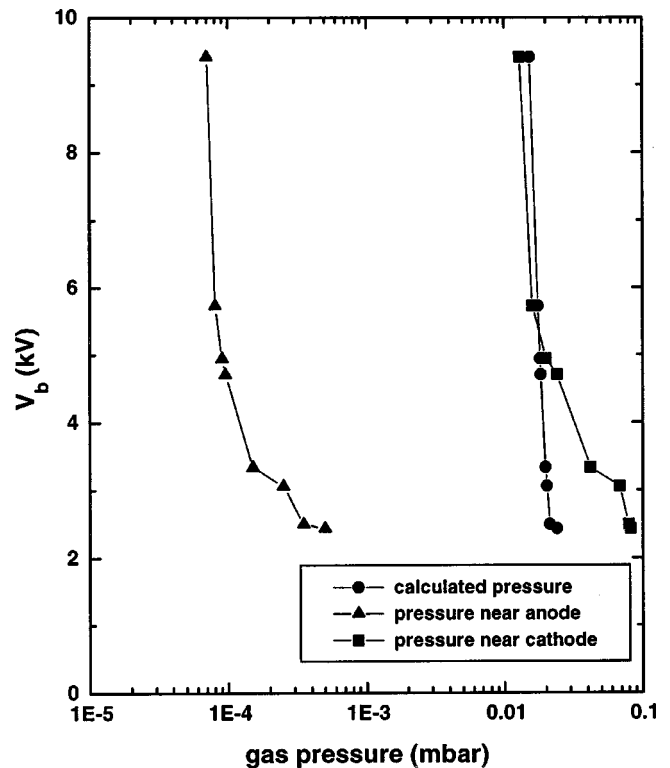


FIG. 13. Left-hand branch for Region I of the Paschen curve.

that this empirical formula, unlike DPPD, corresponds to the case where there is no gas flow.

In Fig. 13, the calculated pressures (Region I) lie closer to the pressure measured near the cathode. However, the available voltage near the cathode (before breakdown) is only one-fifth of the voltage across the main gap. Hence there exists a significant deviation between the calculated pressures and the pressures measured near the anode. Thus the empirical relationship, $V \propto (p^2 d D)^{-2}$, valid for a uniform pressure along the discharge column, is not applicable when the pressure gradient along the discharge column is over two orders of magnitude. Hence, the possibility of an entirely different kind of mechanism prevails in this device.

B. Energetic electrons

The self-biasing collector technique indicates the presence of energetic electrons having a significant spread in energies. The conventional pseudospark discharge plasma is comprised of two electron components,¹⁷ one with energies in the range of 100–400 eV, described as an electron beam that is comprised of the main discharge, and the other with a temperature of typically few eV. The electron beam is obtained in the initial pulse that lasts for few 100 ns that propagates by ionizing the background neutrals.⁵

In the present case several electron current pulses are observed at the collector. This is unlikely in the conventional pseudospark discharge, where the electron beam is formed during the first few 100 ns of the discharge and is subsequently absent. In the present case it is possible that the measured current signal is due to plasma created near the downstream of the anode. This is possible due to the plasma flowing from the device, as well as background ionization of

the gas atoms by the energetic species emitted from the device. Since the energies of the charged species are large to account for the temperature of the plasma, it is most likely that the observed current peaks are admixtures of plasma as well as energetic electrons. The grounded collector behaving as a probe is insensitive in distinguishing them. Such multiple current pulses have also been reported by other authors.¹⁶

C. Possible discharge mechanism

As observed, (Fig. 5) the initial electron current pulse at the grounded collector is small in magnitude when the device is operated in Region I in comparison to Region II (Fig. 6). The above observation gives certain clues to the possible discharge mechanism of this device. If the electron current at the grounded collector is attributed to the admixture of plasma flowing from the device, energetic species, and the background ionization of the neutrals, it is likely that this should be low when the pressure is much lower near the anode (Region I). With a large pressure difference across the discharge electrode, it is possible that discharge initiates somewhere within the discharge column satisfying minimum E/p ratio. In the absence of sufficient neutrals in the background, the plasma density formed near the anode will be weaker resulting in space charge limitation of energetic electrons being emitted from the device. This is not the case when the device is operated in Region II, where the pressure all along the discharge column is in the pseudospark pressure range and is sufficiently higher near the anode. This gives an insight that background plasma is necessary for the extraction of energetic electrons from the device. When operated in Region I, the initial discharge electrons have to ionize the available neutrals near the anode where the pressure is low. Once plasma fills up the entire column at the cost of initial energetic electrons, the successive current pulses are obtained from the discharge. The fall in magnitude of electron current (Figs. 8 and 9) with increasing collector distance from the anode shows certain similarity in this aspect. The initial electron current pulse in this case falls off much faster in comparison to the succeeding current pulses.

More detailed experiments on measuring the potential development at the intermediate electrodes are being carried out to understand the space charge effects along the discharge column. Additional experiments to measure the flow velocity of the gas, pressure variation along the discharge column, and the characterization of downstream plasma including emittance are in progress.

ACKNOWLEDGMENTS

The authors sincerely thank A. K. Chakraborty for discussions and helpful suggestions in organizing this article. The authors also thank H. A. Pathak, Dr. C. Reddy, Dr. K. K. Jain, and Dr. S. K. Mattoo for criticisms and suggestions related to future experiments in this direction. The author would also like to thank the referee whose suggestions have improved the article.

- ¹M. A. Gundersen and G. Schaefer, *Physics and Application of Pseudosparks*, NATO ASI Series, Series B, Physics (Plenum, New York), Vol. 219.
- ²M. T. Ngo, K. H. Schoenbach, G. A. Gerdin, and J. H. Lee, *IEEE Trans. Plasma Sci.* **18**, 669 (1990).
- ³K. K. Jain, E. Boggasch, M. Reiser, and M. J. Rhee, *Phys. Fluids B* **2**, 2487 (1990).
- ⁴M. Gastel, H. Hillmann, F. Muller, and J. Westheide, *IEEE Trans. Plasma Sci.* **23**, 248 (1995).
- ⁵R. Stark, J. Christiansen, K. Frank, and F. Mucke, *IEEE Trans. Plasma Sci.* **23**, 258 (1995).
- ⁶M. Stetter, *IEEE Trans. Plasma Sci.* **23**, 258 (1995).
- ⁷J. Wetheide, *IEEE Trans. Plasma Sci.* **23**, 254 (1995).
- ⁸E. M. Oks, A. V. Vizir, and G. Y. Yushkov, *Rev. Sci. Instrum.* **69**, 853 (1998).
- ⁹M. J. Rhee and E. Boggasch, in Ref. 1, pp. 343–348.
- ¹⁰A. Roth, *Vacuum Technology*, 2nd ed. (Elsevier and North-Holland, Amsterdam).
- ¹¹N. B. Mandache, A. M. Pointu, E. Dewald, M. Nistor, M. Ganciu, G. Musa, and I. I. Popescu, *Plasma Sources Sci. Technol.* **6**, 1 (1997).
- ¹²M. V. Udrea, A. M. Pointu, G. Modreanu, M. Ganciu, I. L. Popescu, and N. B. Mandache, *J. Phys. D* **30**, L33 (1997).
- ¹³H. M. Kudyan, *Rev. Sci. Instrum.* **49**, 8 (1978).
- ¹⁴S. Mukherjee and P. I. John, *IEEE Trans. Plasma Sci.* **23**, 133 (1995).
- ¹⁵C. J. Liu and M.-J. Rhee, *IEEE Trans. Plasma Sci.* **23**, 235 (1995).
- ¹⁶M. Legentil, C. Postel, J. C. Thomaz, Jr., and V. Peuch, *IEEE Trans. Plasma Sci.* **23**, 330 (1995).
- ¹⁷H. Bauer, G. Kirkman, and M. A. Gundersen, in Ref. 1.